THE JOURNAL OF BIOLOGICAL CHEMISTRY VOL. 289, NO. 52, pp. 35711–35723, December 26, 2014


# The Role of Autophagy during Group B *Streptococcus* Infection of Blood-Brain Barrier Endothelium*

Received for publication, June 30, 2014, and in revised form, October 27, 2014 Published, JBC Papers in Press, November 4, 2014, DOI 10.1074/jbc.M114.588657

**Andrew S. Cutting[‡], Yvette Del Rosario[‡], Rong Mu[‡], Anthony Rodriguez[‡], Andreas Till[§¶], Suresh Subramani[§], Roberta A. Gottlieb[‖], and Kelly S. Doran[‡**1]**

*From the [‡]Department of Biology and [‖]Donald P. Shiley BioScience Center, San Diego State University, San Diego, California 92182, [§]Division of Biological Sciences and San Diego Center for Systems Biology, University of California, San Diego, La Jolla, California 92093-0322, [¶]Stem Cell Pathologies Group, Life and Brain Center, University of Bonn, D-53127 Bonn, Germany, and **Department of Pediatrics, University of California San Diego School of Medicine, La Jolla, California 92093*

**Background:** Penetration of brain endothelium by Group B *streptococcus* (GBS) is the first step in the development of meningitis.
**Results:** Autophagy is activated in response to GBS infection.
**Conclusion:** Autophagy induction occurs through GBS toxin expression, while key autophagic proteins contribute to GBS destruction.
**Significance:** Understanding the role of autophagy in brain endothelium may inform novel strategies to prevent the pathogenesis of bacterial meningitis.

**Bacterial meningitis occurs when bloodborne pathogens invade and penetrate the blood-brain barrier (BBB), provoking inflammation and disease. Group B *Streptococcus* (GBS), the leading cause of neonatal meningitis, can enter human brain microvascular endothelial cells (hBMECs), but the host response to intracellular GBS has not been characterized. Here we sought to determine whether antibacterial autophagy, which involves selective recognition of intracellular organisms and their targeting to autophagosomes for degradation, is activated in BBB endothelium during bacterial infection. GBS infection resulted in increased punctate distribution of GFP-microtubule-associated protein 1 light chain 3 (LC3) and increased levels of endogenous LC3-II and p62 turnover, two hallmark indicators of active autophagic flux. Infection with GBS mutants revealed that bacterial invasion and the GBS pore-forming β-hemolysin/cytolysin (β-h/c) trigger autophagic activation. Cell-free bacterial extracts containing β-h/c activity induced LC3-II conversion, identifying this toxin as a principal provocative factor for autophagy activation. These results were confirmed *in vivo* using a mouse model of GBS meningitis as infection with WT GBS induced autophagy in brain tissue more frequently than a β-h/c-deficient mutant. Elimination of autophagy using *Atg5*-deficient fibroblasts or siRNA-mediated impairment of autophagy in hBMECs led to increased recovery of intracellular GBS. However, electron microscopy revealed that GBS was rarely found within double membrane autophagic structures even though we observed GBS-LC3 co-localization. These results suggest that although autophagy may act as a BBB cellular defense mechanism in response to invading and toxin-producing bacteria, GBS may actively thwart the autophagic pathway.**

Bacterial meningitis is a serious infection of the central nervous system (CNS) that can develop rapidly into a life-threatening infection even in previously healthy children or adults. The Gram-positive bacterium *Streptococcus agalactiae*, known as group B *Streptococcus* (GBS),[2] is the leading cause of meningitis in newborn infants (1). Although antibiotic therapy has changed GBS meningitis from a uniformly fatal disease to an often curable one, the overall outcome remains unfavorable as 25–50% of surviving infants suffer permanent neurological sequelae of varying severity, including cerebral palsy, mental retardation, blindness, deafness, and seizures (2). Infection is initiated when bloodborne bacteria cross the blood-brain barrier (BBB) in a complex interplay between endothelial cells and microbial gene products. The human BBB, which is composed of a single layer of specialized human brain microvascular endothelial cells (hBMECs), separates the brain and its surrounding tissues from the circulating blood, tightly regulating the flow of nutrients and molecules promoting the proper biochemical conditions for normal brain function (3, 4). Although the BBB serves as a critical barrier to protect the CNS against microbial invasion, disruption of the BBB is a hallmark event in the pathophysiology of bacterial meningitis. This disruption

* This work was supported, in whole or in part, by National Institutes of Health Grants GM069373 (to S. S.), R01-NS051247 and associated supplement from the NINDS (to A. R. and K. S. D.), and GM085764, a seed grant from the San Diego Center for Systems Biology (to A. T. and S. S.). This work was also supported by a Rees-Stealy Research Foundation/San Diego State University Heart Institute fellowship (to A. S. C.) and Deutsche Forschungsgemeinschaft (German Research Foundation) Fellowship Ti-640 1-1.
[1] To whom correspondence should be addressed: Dept. of Biology and Center for Microbial Sciences, San Diego State University, 5500 Campanile Dr., NLS 317, San Diego, CA 92182. Tel.: 619-594-1867; E-mail: kdoran@mail.sdsu.edu.

[2] The abbreviations used are: GBS, group B *Streptococcus*; BBB, blood-brain barrier; hBMEC, human brain microvascular endothelial cell; β-h/c, β-hemolysin/cytolysin; *iagA*, invasion-associated gene A; ATG, autophagy; LC3, microtubule-associated protein 1 light chain 3; GAS, group A *Streptococcus*; THB, Todd-Hewitt broth; MEF, mouse embryonic fibroblast; m.o.i., multiplicity of infection; TEM, transmission electron microscopy; mTOR, mammalian target of rapamycin; LPA, LC3-associated phagocytosis.

may be due to the combined effect of bacterial entry, direct cellular injury by bacterial cytotoxins, and/or activation of host inflammatory pathways that compromise barrier function. GBS produces a pore-forming β-hemolysin/cytolysin (β-h/c) that has been shown to directly damage brain endothelial cells (5) and activate proinflammatory mediators, promoting the development of GBS meningitis *in vivo* (6, 7). To gain entry into the CNS and the subarachnoid space, GBS must persist in the blood stream and interact with and penetrate brain endothelium; however, the exact mechanism(s) of bacterial transit across the BBB is not known. It is likely that GBS tropism for the BBB is the primary step in the pathogenesis of meningitis. Many GBS surface components have been identified that contribute to the initial interaction with hBMECs, including invasion-associated gene A (*iagA*), which is required for proper anchoring of lipoteichoic acid to the cell wall (8); Srr-1 (9, 10); FbsA (11); Lmb (12); HvgA (13); alpha C protein (14); and pili components, which consist of the pilus backbone protein PilB and pilus tip adhesin PilA (15, 16). GBS is able to enter or "invade" brain endothelium apically and exit the cell on the basolateral side, thereby crossing the BBB transcellularly (5, 7). Electron microscopy (EM) studies have demonstrated the presence of GBS in membrane-bound vesicles within hBMECs (5), suggesting the involvement of endocytic pathways. However, little is known about how GBS persists and traffics through the BBB or the host defenses deployed to combat its intracellular presence in brain endothelium.

Macroautophagy, hereafter referred to as autophagy, is an evolutionarily conserved degradation process that utilizes the lysosomal machinery to recycle damaged, aggregated, or aged cytoplasmic constituents. Cargo is initially captured into the autophagosome through the formation of an isolation membrane called the phagophore, which is ultimately destined for lysosomal fusion resulting in cargo degradation (17, 18). Autophagy is initiated by the interactions between multiple autophagy (ATG) proteins (19). ATG5, ATG12, and microtubule-associated protein 1 light chain 3 (LC3)/GATE-16/GABA receptor-associated protein are vital for the formation of the initial phagophore and maturation of the autophagosome. LC3 is conjugated to phosphatidylethanolamine, a lipid constituent of plasma membranes, by the ATG5-ATG12-ATG16L1 complex to allow for autophagosome expansion (19). Recently, antimicrobial autophagy, a selective type of autophagy also known as xenophagy, has emerged as a potent host defense mechanism against intracellular bacterial and viral pathogens (17, 20). Several pathogenic bacteria such as *Salmonella enterica* serovar Typhimurium (*Salmonella typhimurium*), *Listeria monocytogenes*, *Shigella flexneri*, and group A *Streptococcus* (GAS) have been shown to activate the autophagic pathway (21–23). Multiple mechanisms have been described as to how these and other pathogens are recognized by the cell to induce the autophagic process (24). Further modulation or evasion of these pathways by bacteria may be critical for their intracellular survival and disease manifestation.

In the present study, we examined the hypothesis that selective autophagy may play a role in host defense against meningeal pathogens such as GBS. Our results demonstrate that GBS infection triggers a robust autophagic response in brain endothelium and that this response contributes to limiting intracellular bacteria. Experiments with isogenic GBS mutants lacking the β-h/c toxin or surface components that promote cellular invasion indicate that these virulence factors impact autophagy induction. Furthermore, our studies demonstrate that the GBS-secreted β-h/c toxin is sufficient to activate an acute autophagic response in BBB endothelium but that this response may not be adequate to reduce the majority of intracellular GBS.

## EXPERIMENTAL PROCEDURES

*Bacterial Strains*—The WT strains used in these studies include *Bacillus anthracis* (Sterne 7702) (25) and *Staphylococcus aureus* (ISP479C) (26) and clinical GBS isolates COH1, a highly encapsulated serotype III strain, and NCTC 10/84, a highly hemolytic serotype V strain (27, 28). Mutant GBS strains COH1Δ*cylE* (29), NCTC10/84Δ*cylE* (29), COH1Δ*iagA* (8), NCTC10/84Δ*pilA* (16), and NCTC10/84Δ*pilB* (30) were constructed previously by single gene allelic exchange mutagenesis as described. All GBS strains were grown in Todd-Hewitt broth (THB) with antibiotic selection, 2 μg/ml chloramphenicol or 5 μg/ml erythromycin, as needed. The *B. anthracis* Sterne strain and the methicillin-sensitive *S. aureus* ISP479C strains were cultured as described previously (31, 32).

*Construction of Green Fluorescent Protein-expressing GBS*—The pDESTerm plasmid expressing GFP was provided by John Buchanan and Victor Nizet (University of California, San Diego). Competent bacterial cells were created by propagating GBS in THB with 0.6% glycine to early log phase. Cells were then centrifuged at 4000 rpm for 30 min at 4 °C. The supernatant was removed, and bacteria were washed with ice-cold 0.625 M sucrose buffer. Bacteria were centrifuged again as described above, and again the supernatant was removed. 1 μg/μl plasmid was added to the competent GBS in a 0.1-cm electroporation cuvette, and cells were electroporated at 1500 V for 2–4 ms. All steps were performed on ice. Recovery medium (THB with 0.25 M sucrose) was added to the cells, and cells were incubated at 37 °C for 1 h. The culture was then plated on THB agar plates containing 5 μg/ml erythromycin and incubated at 37 °C with 5% $CO_2$. Colonies were then assessed for fluorescence by microscopy and fluorescent-activated cell sorting.

*Cell Culture*—The human brain microvascular endothelial cell line was kindly provided by Kwang Sik Kim (The Johns Hopkins University) and cultured as described previously in RPMI 1640 medium (VWR, catalog number 45000-396) containing 10% FBS, 10% Nuserum (BD Biosciences, catalog number 355504), and 1% nonessential amino acids (Invitrogen, catalog number 11140-050) (33). ATG5−/− and WT mouse embryonic fibroblasts (MEFs) (34) were kindly provided by Noboru Mizushima (University of Tokyo) and cultured in DMEM plus GlutaMAX containing 10% FBS and 1% penicillin/streptomycin (35). For RNAi-mediated gene knockdown, siRNAs directed toward ATG12 (Invitrogen Select Silencer Series, catalog number 4392420, s17465 and s17466), ATG5 (Invitrogen Select Silencer Series, catalog number 4392420, s18159 and s18160), FIP200 (Qiagen, catalog numbers SI02664571 and SI02664578), and a scrambled siRNA (Invitrogen Select Silencer Series, catalog number 4390846) were used.

hBMECs were transfected with either siATG12, siATG5, siFIP200, or siRNA scrambled control for 2 days with Lipofectamine 2000 (Invitrogen, catalog number 11668-019) or Lipofectamine 3000 (Invitrogen, catalog number L3000-001) prior to GBS infection. Knockdown of target genes was confirmed by immunoblotting. mCherry-LC3 has been described previously (36); briefly, the pEGFP-C1 vector (Addgene) was modified by replacement of enhanced GFP with mCherry, and LC3 was inserted at the C terminus.

*Infection Assays*—hBMECs and ATG5 knock-out (KO) and WT MEFs were grown to confluence (~$10^5$ cells/well) and washed three times prior to GBS infection. GBS was grown in THB to midlog phase (~$10^8$ cfu/ml; $A_{600}$ = 0.4), washed in PBS, resuspended in RPMI 1640 medium plus 10% FBS, and used to infect monolayers at a multiplicity of infection (m.o.i.) of 1 or 10 for various time points. Plates were then centrifuged at 1000 rpm for 3 min to synchronize infection and incubated at 37 °C in 5% $CO_2$. After infection, cells were treated with penicillin (5 $\mu$g/ml) and gentamycin (100 $\mu$g/ml) to kill extracellular GBS for various time points. Cells were treated with 0.1 ml of 0.25% trypsin, EDTA solution and lysed with addition of 0.4 ml of 0.025% Triton X-100 by vigorous pipetting. The lysates were then serially diluted and plated on THB agar to enumerate bacterial cfu. Cell lysate was collected and stored at −80 °C until further use. In specified experiments, hBMECs were pretreated with rapamycin (5 $\mu$M; Calbiochem, catalog number 553211) and bafilomycin (100 nM; LC Laboratories, catalog number B-1080) for 1 h prior to GBS infection.

*Transmission Electron Microscopy*—hBMECs were incubated with GBS at 37 °C with 5% $CO_2$. Cells were washed three times with PBS. Cells were fixed with 2.5% glutaraldehyde in 0.1 M cacodylate buffer for 90 min and rinsed 3 times in 0.1 M cacodylate buffer for 10 min for each rinse. Samples were post-fixed in 1% osmium tetroxide for 90 min and then dehydrated at increasing concentrations of ethanol and acetone for 10 min each. Samples were embedded in Epon acetone and baked at 60 °C overnight. Thin sections were cut using a diamond knife on a Leica microtome, stained with uranyl acetate and lead citrate, and viewed using an FEI Tecnai 12 transmission electron microscope.

*Immunofluorescence Staining*—hBMECs were fixed with 4% paraformaldehyde prior to mounting with VectaShield with DAPI (Vector Laboratories, catalog number H-1200). For GFP-LC3 studies, hBMECs were transduced with GFP-LC3 adenovirus overnight in RPMI 1640 medium containing 2% FBS before infection with GBS. After infection, cells were fixed in 4% paraformaldehyde prior to solubilization in 0.1% Triton X-100 and subsequent staining with a GBS-specific antibody (Acris, catalog number BM5557P) or anti-von Willebrand factor antibody (Sigma, catalog number F3520). For tissue visualization of GFP-LC3 mice, brains were harvested and fixed in optimal cutting temperature compound (O.C.T.) (VWR, catalog number 25608-930) and then frozen at −80 °C. Brain tissue was then sectioned using a Leica cryostat. Samples were visualized using a Zeiss Axiovert 200 inverted fluorescence microscope (Carl Zeiss) or a Zeiss LSM 710 confocal microscope (Carl Zeiss).

*Western Blot Analysis*—hBMECs were infected with WT and mutant GBS for different time points and lysed using radioimmune precipitation assay buffer (Thermo Scientific, catalog number 89900) containing 100 mM NaF, 10 mM sodium pyrophosphate, 1 mM PMSF, and protease inhibitor mixture III (Calbiochem, catalog number 539134-1ML). Cell lysates (10 $\mu$g) were separated by SDS-PAGE performed with 10–20% tris-glycine gels (Invitrogen, catalog number EC6135BOX) and then transferred to PVDF membranes (Millipore, catalog number IPVH00010), blocked using Tris buffer (pH 7.6) containing 0.1% Tween 20 with 5% (w/v) nonfat dry milk. Blots were then incubated overnight with antibodies against LC3 (1:2000; Cell Signaling Technology, catalog number 4108), GAPDH (1:150,000; Millipore, catalog number MAB374), ATG12 (1:1000; Cell Signaling Technology, catalog number 2010), ATG5 (1:500; Santa Cruz Biotechnology, catalog number sc-133158), p62 (1:1000; Santa Cruz Biotechnology, catalog number sc-28359), or FIP200 (1:1000; Cell Signaling Technology, catalog number 12436) in blocking buffer at 4 °C followed by detection with peroxidase-conjugated goat anti-rabbit IgG (1:1000; Jackson ImmunoResearch Laboratories, catalog number 111-035-003) and donkey anti-mouse IgG (1:1000; Jackson ImmunoResearch Laboratories, catalog number 715-035-150). Western blots were developed with WesternBright ECL HRP substrate (Advansta, catalog number K12045-D20).

*Preparation of Heat-killed and Paraformaldehyde-fixed GBS*—Bacteria were grown to midlog phase in THB and subsequently pelleted. Pelleted bacteria were reconstituted in PBS and then boiled at 95 °C for 5 min. After boiling, bacteria were diluted accordingly for an m.o.i. of 10 and administered to hBMECs. For paraformaldehyde fixation, bacteria were grown to midlog phase in THB, pelleted, resuspended in 1% paraformaldehyde, and incubated for 10 min at room temperature. The fixed pellet was then washed three times with PBS and added to hBMECs at an m.o.i. of 10.

*Preparation of GBS Hemolytic Extract*—GBS hemolytic extract was prepared as described previously (6, 37). Briefly, WT GBS NCTC 10/84 and isogenic Δ*cylE* strains were grown to an $A_{600}$ of 0.4–0.6 in THB. Bacteria were then pelleted and resuspended in PBS containing 1% glucose and 1% starch. After 1 h at room temperature, bacteria were sterile filtered using a 0.2-$\mu$m syringe filter. After filtration, bacteria were pelleted and washed once in PBS. The washed pellet was then incubated for 1 h at 37 °C. The bacteria were then pelleted and resuspended in PBS plus 1% starch and 1% glucose, and the supernatant was sterile filtered using a 0.2-$\mu$m syringe filter. And equal volume of ice-cold methanol was added to the filtered supernatant and incubated on ice for 1 h. Methanol/supernatant was then pelleted and resuspended in 1 ml of PBS. The hemolytic titer of the isolated extract was quantified as described previously (38).

*Mouse Model of Hematogenous Meningitis*—Animal experiments were approved by Institutional Animal Care and Use Committee at San Diego State University Protocol APF 13-07-011D and performed using accepted veterinary standards. We utilized a mouse model of hematogenous GBS meningitis as described previously (6, 8, 15). 8-week-old male CD-1 mice ($n$ = 10) were injected intravenously with 7–8 × $10^7$ cfu of

NCTC 10/84 GBS or isogenic Δ*cylE* mutant. At the time of morbidity or the experimental end point (24 h), mice were euthanized, and blood and brain were collected. One half of the brain was homogenized and processed for Western blot analysis in radioimmune precipitation assay buffer, and the other half was homogenized and plated on THB agar plates for enumeration of cfu. GFP-LC3 transgenic mice (39) (aged 10–12 weeks) were similarly infected with WT GBS or the Δ*cylE* mutant ($n = 3$) or injected with PBS control, and at the experimental end point (24 h), brain tissue was isolated and cryopreserved in optimal cutting temperature (O.C.T.) compound prior to immunofluorescence microscopy.

*Statistical Analyses*—GraphPad Prism version 5.0f was used for statistical analysis. Unpaired *t* tests or one-way analysis of variance was used for analysis. Statistical significance was accepted at $p < 0.05$.

## RESULTS

*Bacterial Infection Induces Autophagy in Brain Endothelial Cells*—To investigate autophagy activation in hBMECs, we analyzed the processing and lipidation of LC3. Upon initiation of autophagy, the cytosolic LC3-I form is converted to LC3-II, which is covalently linked to phosphatidylethanolamine and associated with autophagosomal membranes (40). Ectopically expressed LC3, which is N-terminally tagged with GFP (GFP-LC3), is diffusely distributed in the cytosol, but upon proteolysis of the C terminus and lipidation, it is recruited into autophagosomes, which are evident as fluorescent puncta. Initially, we infected hBMECs with known meningeal pathogens that are capable of invading brain endothelial cells, including GBS (5), *B. anthracis* (31), and *S. aureus* (32). Following transduction of hBMECs with an adenovirus expressing GFP-labeled LC3 (Ad-GFP-LC3) (41) and subsequent bacterial infection, we observed a significant number of LC3 puncta compared with the uninfected control (Fig. 1*A*). We further examined two well studied GBS clinical isolates shown to cause experimental meningitis, COH1 (serotype III) and NCTC 10/84 (serotype V) (6, 10). Increased formation of LC3 puncta can be visualized after COH1 WT GBS infection in comparison with an uninfected control (Fig. 1*B*). Furthermore, Western blot analysis of endogenous LC3 levels in hBMECs during infection revealed a significant increase in LC3-II levels compared with LC3-I at early time points (Fig. 1, *C* and *D*). We also investigated the turnover of the autophagic adaptor protein p62/sequestome-1 (42), which interacts with LC3 and is an indicator of active autophagy (43–47). We observed an early decrease in p62 compared with the cytosolic marker GAPDH following GBS infection (Fig. 1, *C* and *D*), which is consistent with autophagic flux. Furthermore, analysis of our previously obtained data on the hBMEC transcriptional response following GBS infection (15) revealed a number of modulated genes within autophagy gene networks, including *Atg10* and *Xbp1* (data not shown). Collectively, these data indicate that autophagy in BBB endothelium is activated early during pathogen infection.

*Bacterial Invasion and Toxin Production Activate Autophagy*—To test whether GBS must be actively replicating to induce autophagy, we incubated hBMECs with heat-killed or paraformaldehyde-fixed GBS. As shown in Fig. 2, *A–D*, neither heat-killed nor paraformaldehyde-fixed bacteria were able to induce substantial LC3-II conversion or p62 turnover compared with infection with live GBS. These data demonstrate that live bacterial infection is required to induce autophagy in brain endothelium, which may involve active bacterial transcription and protein synthesis and/or bacterial uptake into host cells. We next examined a subset of GBS virulence factors known to play a role in the pathogenesis of meningitis, specifically those involved in hBMEC attachment and invasion and in toxin production. Using GBS mutant strains lacking *cylE*, which codes for β-h/c activity, and pili components *pilA* and *pilB*, which promote GBS interaction with hBMECs, we assessed their ability to induce autophagy in BBB endothelium. Infection with the Δ*pilA* and Δ*pilB* mutants induced LC3-II conversion and p62 turnover similar to those of WT GBS, whereas strains lacking the β-h/c toxin resulted in less LC3-II (Fig. 2, *E* and *F*). Similar results were observed for a Δ*cylE* mutant in a different GBS WT parental background (Fig. 2, *G* and *H*). Additionally, the GBS Δ*iagA* mutant, which exhibits reduced bacterial invasion (8), resulted in less LC3-II conversion. We sought to further investigate the role of the β-h/c toxin in autophagy activation in brain endothelium. Compared with the WT strain, the GBS mutant lacking the β-h/c toxin induced significantly less LC3 puncta (Fig. 3, *A* and *B*) and reduced endogenous levels of LC3-II as well as increased p62 (Fig. 3, *C*, *D*, and *E*). These data suggest that GBS toxin production is required for autophagy activation in brain endothelium.

To determine whether the β-h/c toxin could independently induce autophagy in hBMECs, cell-free extracts from GBS were prepared in PBS plus 2% starch to extract stabilized β-h/c activity from the bacterial surface as described previously (6, 37). Hemolytic titers were determined and were similar to that observed previously (data not shown). hBMEC monolayers were incubated with cell-free extracts from either WT or β-h/c mutant strains. As shown in Fig. 4, *A–C*, extracts containing β-h/c induced LC3-II conversion and p62 turnover in a dose-dependent fashion, whereas extracts from a β-h/c mutant did not result in autophagy activation, indicating that other secreted GBS products had negligible stimulatory effects. Under these experimental conditions, the β-h/c extract did not result in substantial cell death (Fig. 4*D*). These data indicate that brain endothelium responds directly to the GBS β-h/c to activate autophagy pathways independent of live bacterial challenge.

*The GBS β-h/c Promotes Autophagy Activation in Vivo*—Our results suggested a prominent role for the GBS β-h/c toxin in promoting an autophagic response in brain endothelium. To test this hypothesis *in vivo*, we used our murine model of GBS hematogenous meningitis as described previously (6). Groups of mice ($n = 9$) were infected intravenously with WT GBS (NCTC 10/84) or the isogenic Δ*cylE* mutant. As we have demonstrated previously (6, 37), the majority of WT-infected mice died and exhibited high bloodstream and brain bacterial loads compared with Δ*cylE*-infected mice (Fig. 5, *A* and *B*). At the time of death or sacrifice, brains were harvested and processed to obtain protein lysates for subsequent Western blot analysis of LC3 and p62 proteins. We observed increased LC3-II and a concomitant decrease in p62 in the majority of WT GBS-in-

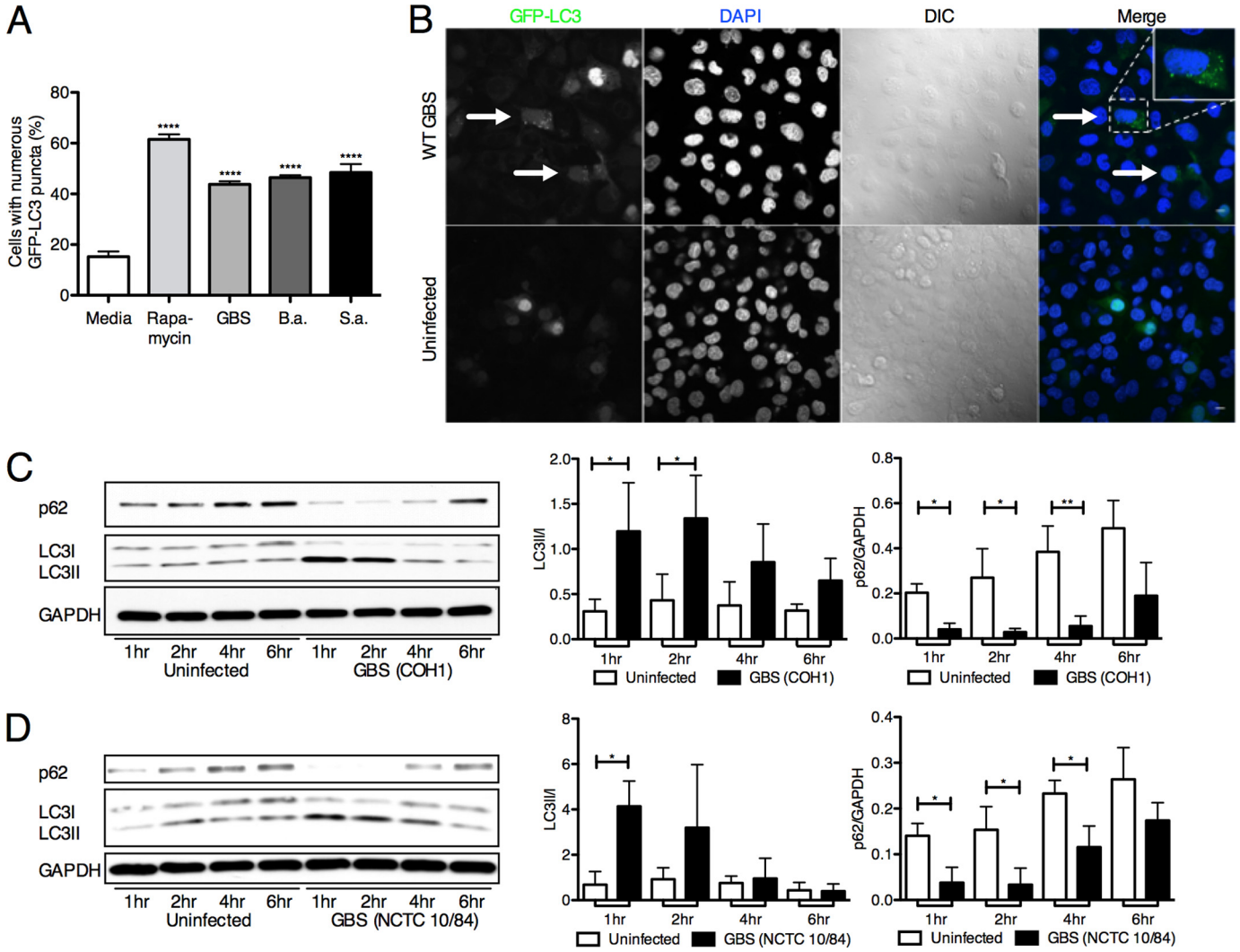


FIGURE 1. **Autophagy induction in hBMECs.** *A*, GFP-LC3 (Ad-GFP-LC3) counts in hBMECs following infection with GBS (COH1 WT), *B. anthracis* (*B.a.*) (Sterne 7702 WT), and *S. aureus* (*S.a.*) (ISP479C WT) for 3 h (m.o.i. = 10) compared with untreated controls. At least 200 cells with numerous puncta were counted, and rapamycin treatment (5 $\mu$M) was used as a positive control. Significance was measured in comparison with untreated controls. *B*, confocal microscopy visualization of COH1 WT and uninfected hBMECs transduced with GFP-LC3. *Arrows* denote cells with abundant amounts of puncta. *Scale bar*, 10 $\mu$m. *C* and *D*, Western blot analysis of LC3 and p62 in hBMEC samples at various time points postinfection with COH1 for 4 h (m.o.i. = 10) and NCTC 10/84 for 1 h (m.o.i. = 10). Image analysis was performed using ImageJ software to determine LC3-II/LC3-I and p62/GAPDH ratios. All experiments were repeated at least three times in triplicate; data represent the mean ± S.D. from a representative experiment. *, $p < 0.05$; **, $p < 0.005$; ****, $p < 0.0001$. *Error bars* represent S.D. *DIC*, differential interference contrast.

fected mice compared with mice infected with the Δ*cylE* mutant (Fig. 5, *C* and *D*). We also similarly infected GFP-LC3 transgenic mice (48) with WT or Δ*cylE* mutant strains. Fluorescence microscopy of representative brains revealed increased GFP-LC3 puncta in brain tissue following GBS WT infection compared with mutant infection or PBS injection (Fig. 6*A*). Additionally, we observed that GBS co-localized with GFP-LC3 within endothelial structures (Fig. 6*B*) and that GFP-LC3 co-localized with von Willebrand factor, a marker of endothelial cells (Fig. 6*C*). These results confirm that autophagy is activated in response to GBS infection and the β-h/c toxin *in vivo*.

*Autophagy Contributes to Bacterial Clearance*—To examine the importance of autophagic activation in combating intracellular GBS, we first used an MEF cell line that is deficient in ATG5 (35). This protein is required for autophagy initiation, and cell lines lacking ATG5 are not able to form the ATG5-ATG12-ATG16L1 initiation complex required to elongate the developing autophagosome (35). Following GBS infection and antibiotic treatment to remove extracellular bacteria (see "Experimental Procedures"), intracellular GBS was enumerated in WT and ATG5 KO MEFs. In the absence of ATG5, significantly more intracellular GBS was recovered (Fig. 7*A*). To establish the protective role of autophagy in brain endothelium, we first pretreated hBMECs with rapamycin, which is known to induce autophagy through its ability to inhibit the protein kinase mTOR complex 1, a pivotal negative regulator of autophagy (49–51). The intracellular bacterial load after pretreatment with rapamycin was significantly lower than in untreated controls (Fig. 7*B*). This suggests that stimulation of autophagy in hBMECs limits GBS intracellular survival. We also utilized bafilomycin A1, an antibiotic known to inhibit autophagosome-lysosome fusion (52), and observed that bafilomycin pretreatment led to a significant increase in the num-

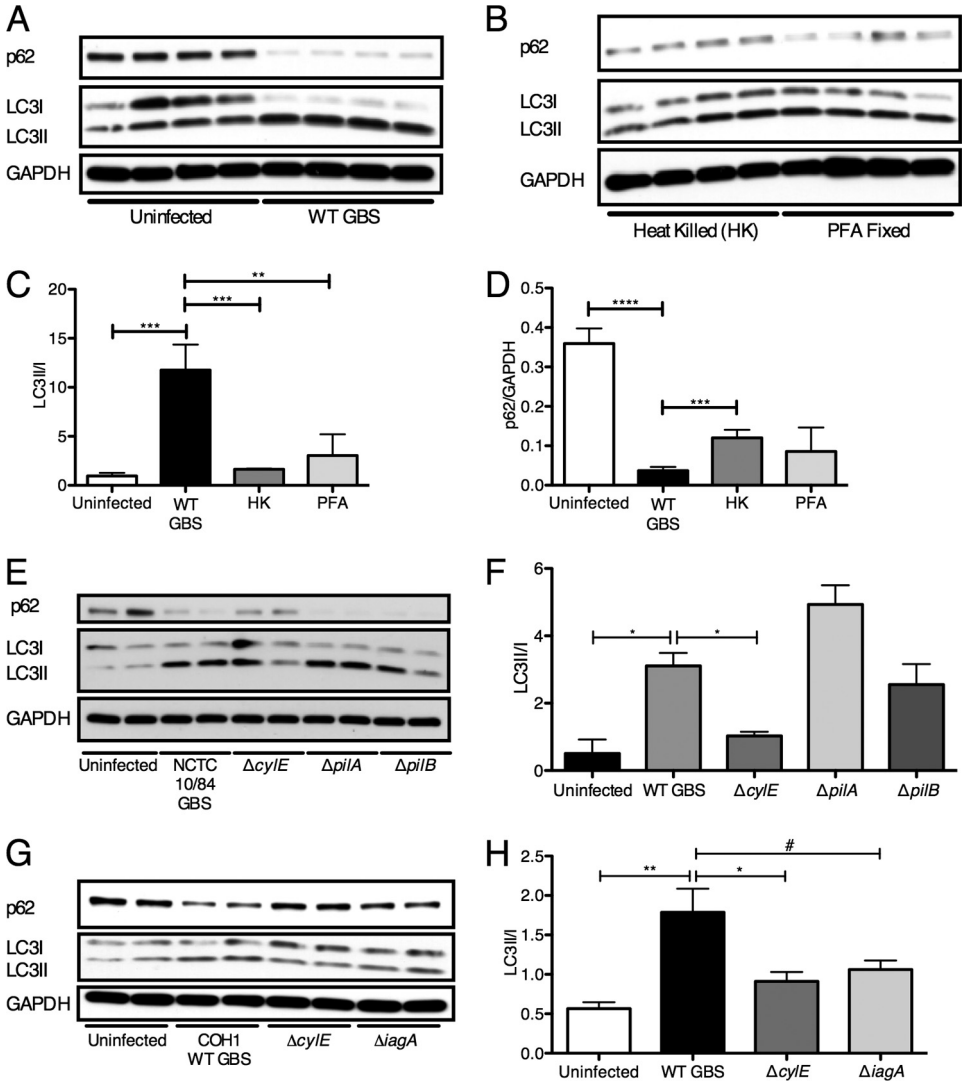


FIGURE 2. **Live bacterial challenge is required for autophagy induction in hBMECs.** *A* and *B*, Western blot analysis was performed in triplicate on hBMEC lysates following infection for 2 h with WT NCTC 10/84 (m.o.i. = 10) and incubation with heat-killed (*HK*) or paraformaldehyde (*PFA*)-fixed GBS. *C* and *D*, image analysis was performed using ImageJ software to determine LC3-II/LC3-I and p62/GAPDH ratios. *E*, Western blot analysis was performed in triplicate on hBMEC lysates following GBS infection for 1 h (m.o.i. = 10) with WT NCTC 10/84 and isogenic mutants Δ*cylE*, Δ*pilA*, and Δ*pilB*. *F*, image analysis was performed using ImageJ software to determine LC3-II/LC3-I ratios from a representative experiment performed in quadruplicate. *G*, Western blot analysis was performed on hBMEC lysates following GBS infection for 4 h (m.o.i. = 10) with WT COH1 and isogenic mutants Δ*cylE* and Δ*iagA*. *H*, image analysis was performed using ImageJ software to determine LC3-II/LC3-I ratios. All experiments were repeated at least three times in triplicate; data represent the mean ± S.D. from a representative experiment. *, $p < 0.05$; **, $p < 0.005$; ***, $p < 0.0005$; ****, $p < 0.0001$; #, $p = 0.05$. *Error bars* represent S.D.

ber of intracellular GBS cfu recovered (Fig. 7*B*). To corroborate these data, we utilized siRNAs directed toward ATG5 and ATG12 to inhibit autophagy in hBMECs during GBS infection. During treatment with siATG5, we observed reduced levels of ATG5 and LC3-II conversion during GBS infection and a slight, although significant, increase in recovered intracellular GBS compared with treatment with the siRNA scrambled control (Fig. 6, *C* and *F*). Similar results were obtained when ATG12 was silenced in hBMECs (Fig. 6, *D* and *G*). To further examine elimination of genes critical for autophagy activation but not LC3 functionality, we knocked down FIP200, a ULK1-interacting protein essential for autophagy induction (53). We observed that knockdown of FIP200 did not similarly result in increased recovery of intracellular GBS (Fig. 3, *E* and *H*). These results suggest that LC3 recruitment and ensuing activation are key contributors to limiting intracellular GBS survival.

*Visualization of Intracellular GBS*—Thus far our results suggest that although the autophagic pathway is activated in brain endothelium during GBS infection, it may play a limited role in reducing the intracellular pool of GBS. Thus we sought to determine whether GBS was found in double membrane structures, which are characteristic of autophagosomes. Using transmission electron microscopy (TEM) analysis, we observed that GBS resides primarily in single membrane-bound compartments within hBMECs and was never free in the cytoplasm at 4 h (Fig. 8*A*) and up to 24 h (data not shown) postinfection. Single membrane structures were often damaged, and a small population had double or multiple membranes (Fig. 8, *A* and *B*). Using confocal microscopy, we further analyzed GBS co-localization with LC3 in hBMECs over time as described under "Experimental Procedures." By 4 h, we observed that ~40% of intracellular GBS co-localized with LC3 (Fig. 8, *C* and *D*), sug-

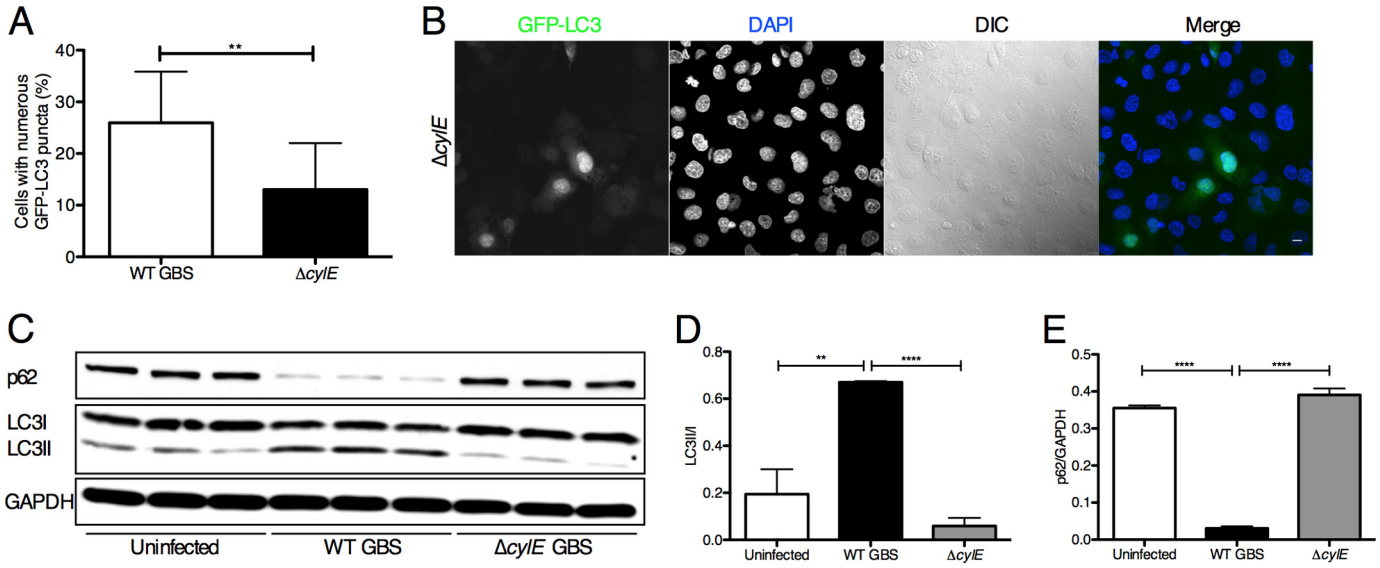


FIGURE 3. **GBS β-h/c triggers autophagy in hBMECs.** *A* and *B*, immunofluorescence of GFP-LC3 (Ad-GFP-LC3) in hBMECs following infection with WT COH1 and isogenic Δ*cylE* mutant for 1 h (m.o.i. = 1). At least 200 cells were counted for puncta, and data are means ± S.D. from a representative experiment performed in triplicate. *Scale bar*, 10 μm. *C*, *D*, and *E*, Western blot analysis was performed on cell lysates collected from hBMECs infected with NCTC 10/84 GBS and isogenic Δ*cylE* mutant for 1 h (m.o.i. = 10) compared with uninfected control. Image analysis was performed using ImageJ software to determine LC3-II/LC3-I and p62/GAPDH ratios. All experiments were repeated at least three times in triplicate; data represent the mean ± S.D. from a representative experiment. **, $p < 0.005$; ****, $p < 0.0001$. *Error bars* represent S.D. *DIC*, differential interference contrast.

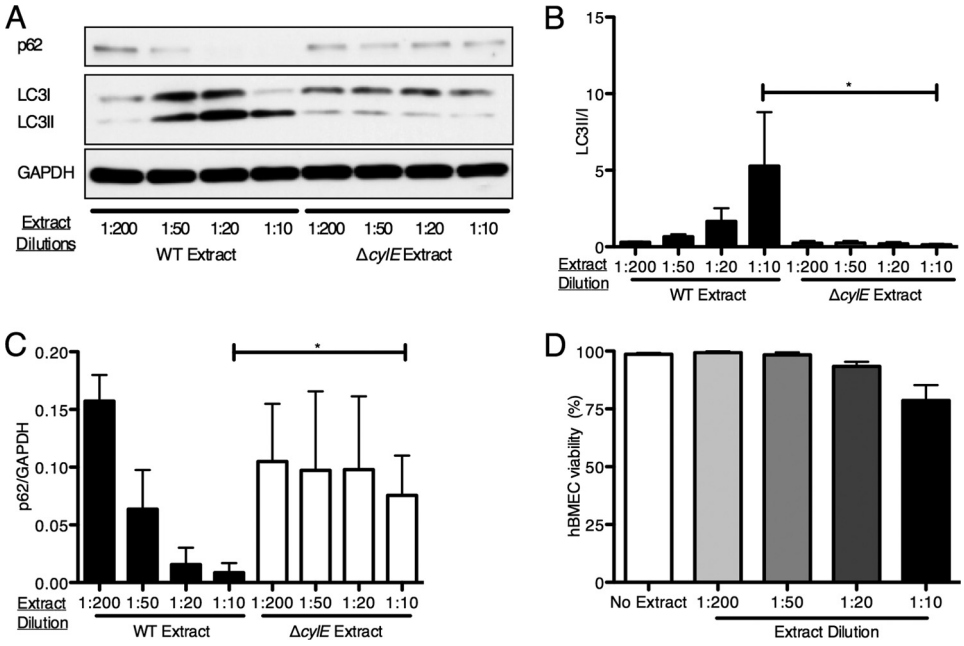


FIGURE 4. **GBS β-h/c extract independently activates autophagy.** *A*, Western blot analysis was performed on cell lysates collected from hBMECs incubated for 2 h with the indicated dilutions of cell-free β-h/c extracts recovered from NCTC 10/84 WT or the isogenic Δ*cylE* mutant. *B* and *C*, image analysis was performed using ImageJ software to determine LC3-II/LC3-I and p62/GAPDH ratios. *D*, hBMECs were incubated with the indicated dilutions of cell-free β-h/c extracts recovered from NCTC 10/84 WT for 2 h and then stained with trypan blue to measure cell viability. All experiments were repeated at least three times in triplicate; data represent the mean ± S.D. from a representative experiment. *, $p < 0.05$. *Error bars* represent S.D.

gesting that less than half of the intracellular pool may be shuttled into the autophagic pathway.

## DISCUSSION

To penetrate the CNS, bacterial pathogens may directly invade BBB endothelium and traverse the barrier in a process called transcytosis. We and others have demonstrated that meningeal pathogens, including GBS, are capable of transcellular passage, but the exact mechanisms of intracellular survival and trafficking are not well understood. It is likely that intracellular host defenses may be activated to combat invasive bacteria, but it is unknown whether autophagy in brain endothelium represents an important BBB defense mechanism or whether meningeal pathogens ultimately thwart or utilize this pathway for survival and BBB traversal. Our results provide new evidence that autophagy/xenophagy is activated in brain endothelium during GBS infection and contributes to limiting intracellular organisms. We demonstrate that inactivation of ATG5

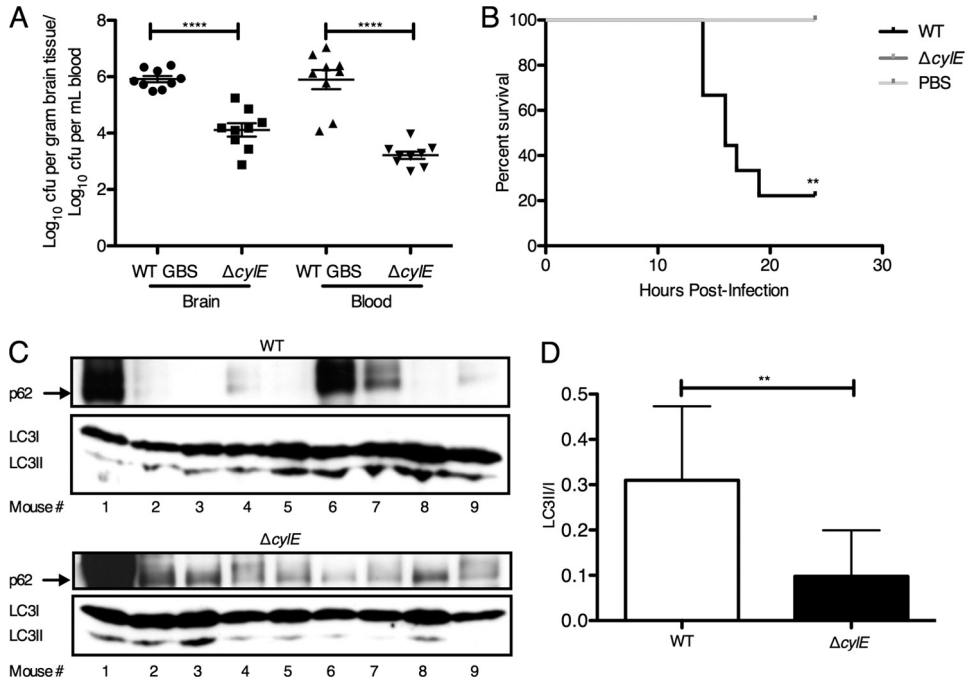


FIGURE 5. **Autophagy is induced *in vivo* following GBS infection.** CD1 male mice were injected intravenously with WT ($n = 9$) or Δ*cylE* GBS strain ($n = 9$) or injected with PBS ($n = 2$). *A*, bacterial counts (cfu) in mouse brain and in blood at the time of death. *B*, Kaplan-Meier survival plot. Significance was assessed using a log rank (Mantel-Cox) test. *C*, Western blot analysis was performed on protein lysates from brain harvested from mice infected with NCTC 10/84 and isogenic Δ*cylE* mutant for LC3-I, LC3-II, and p62. *D*, image analysis was performed using ImageJ software to determine LC3-II/LC3-I ratios. **, $p < 0.005$; ****, $p < 0.0001$. *Error bars* represent S.D.

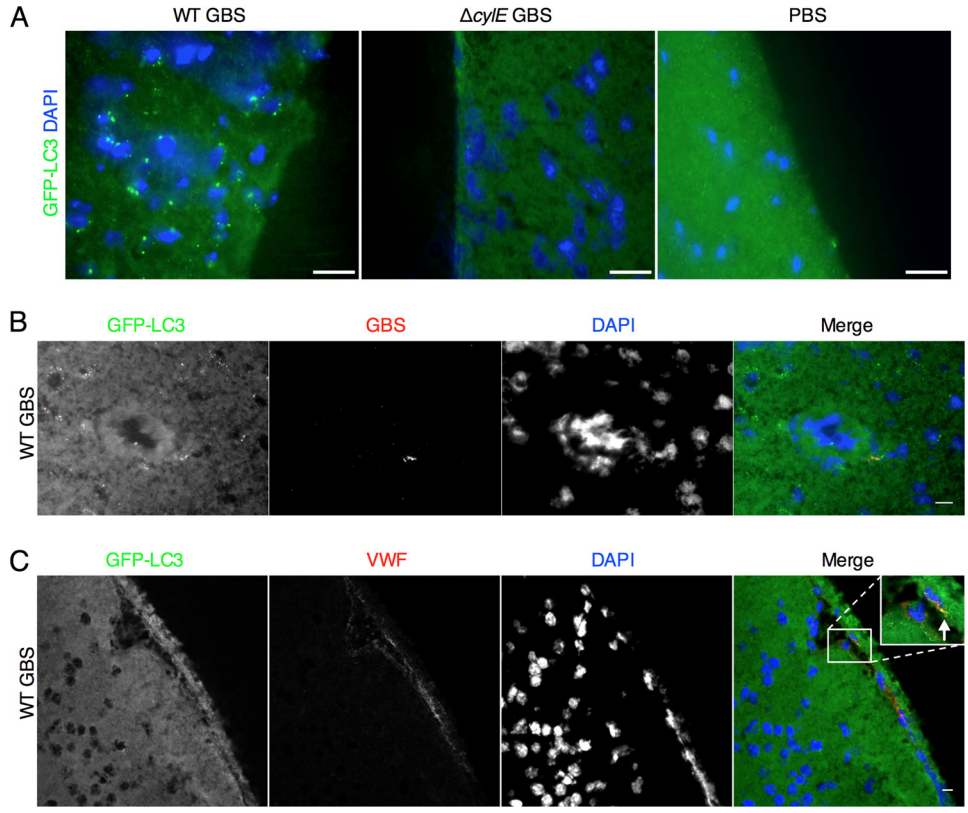


FIGURE 6. **Visualization of autophagy activation in brain endothelium.** *A*, representative brain samples from GFP-LC3 transgenic mice infected with NCTC 10/84 GBS and isogenic Δ*cylE* mutant. GFP-LC3 puncta were observed in brain tissue in WT-infected mice compared with mice infected with the Δ*cylE* mutant or injected with PBS. *Scale bar*, 20 μm. *B*, immunofluorescence for GBS in WT-infected GFP-LC3 transgenic mice. GBS co-localizes with GFP-LC3 within endothelial portions of the brain. *Scale bar*, 10 μm. *C*, immunofluorescence for von Willebrand factor (*VWF*) in GFP-LC3 transgenic WT-infected mice demonstrates that endothelial cells are producing active GFP-LC3. *Scale bar*, 10 μm.

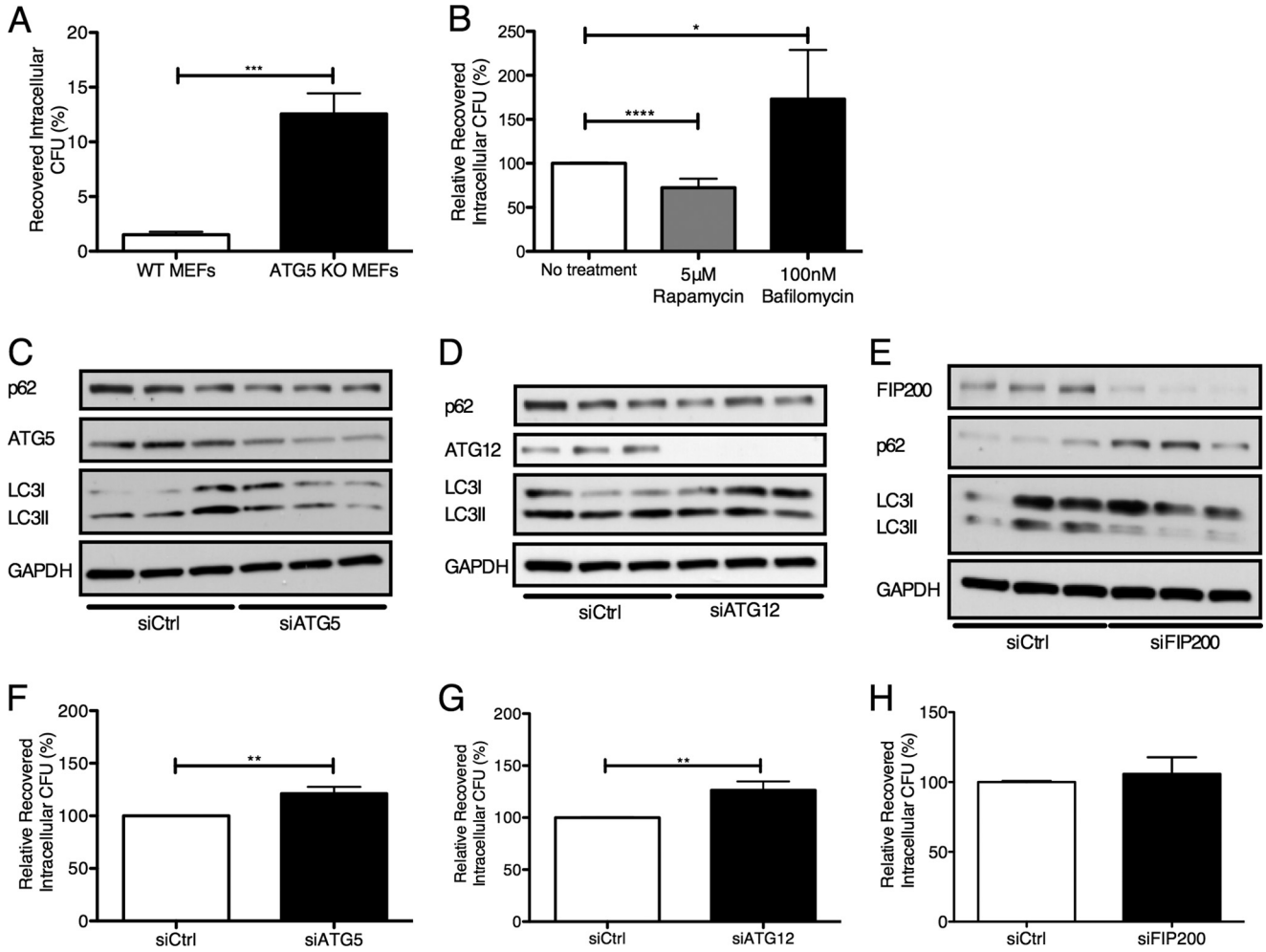


FIGURE 7. **Modulation of autophagy leads to differential GBS intracellular survival.** *A*, recovery of intracellular GBS COH1 within WT and ATG5 KO MEFs following an initial 2-h infection (m.o.i. = 1) and incubation with extracellular antibiotics for 4 h. Invasive bacteria were recovered and are expressed as a percentage of the initial inoculum. *B*, recovery of intracellular GBS NCTC 10/84 following 1-h infection (m.o.i. = 10) in the presence of rapamycin and bafilomycin A1 at 5 $\mu$M and 100 nM, respectively. Recovered bacteria are expressed as a percentage relative to untreated controls. *C*, *D*, *E*, *F*, *G*, and *H*, siRNA knockdown of ATG5, ATG12, and FIP200 in hBMECs was performed as described under "Experimental Procedures." Western blot analysis was performed in triplicate on hBMEC lysates following COH1 WT infection (m.o.i. = 10) for 4 h plus 1-h incubation with extracellular antibiotics. Recovery of intracellular GBS COH1 WT following 4-h infection (m.o.i. = 10) and treatment with extracellular antibiotics for 1 h in the presence of siATG5, siATG12, and siFIP200 is expressed as a percentage relative to cells treated with siRNA scrambled control (*siCtrl*). Data are means ± S.E. from three independent experiments performed in triplicate. *, $p < 0.05$; **, $p < 0.005$; ***, $p < 0.0005$; ****, $p < 0.0001$. *Error bars* represent S.E.

and ATG12, two key autophagy proteins involved in LC3 processing and autophagosome formation, resulted in increased GBS survival. Conversely, we observed that activation of autophagy using rapamycin prior to GBS infection restricts the recovery of intracellular bacteria. Analysis of various GBS mutants deficient in factors previously determined to play a role in disease pathogenesis led to the discovery of the $\beta$-h/c toxin as a key virulence factor associated with autophagy activation. Our data suggest that $\beta$-h/c secretion is sufficient to promote an autophagic response in brain endothelium, a response that is aimed to potentially eliminate intracellular GBS.

Our results demonstrate that hBMECs respond to GBS infection with a robust autophagic response as we observed activation of LC3 and autophagic clearance of the key autophagy adaptor protein p62. Activation was dependent on live bacteria as heat-killed or formalin-fixed GBS failed to induce conversion to LC3-II (Fig. 2, *A*–*D*). This led us to investigate which bacterial virulence determinants may be responsible for autophagy activation in BBB endothelium. We observed that factors associated with GBS invasion into hBMECs such as properly anchored lipoteichoic acid may contribute to autophagy activation. We also found that production of the GBS $\beta$-h/c toxin was an important contributor to autophagy activation in hBMECs. This is a well characterized GBS virulence factor shown to promote GBS invasion and intracellular survival in a variety of cell types as well as immune activation and disease progression (6, 37, 54, 55). Compared with WT GBS infection, we found that infection with a $\beta$-h/c-negative mutant resulted in significantly less autophagy induction in hBMECs *in vitro* and in brain tissue of infected mice. Activation appears to not require bacterial invasion or even the bacterial cell itself as extracts containing $\beta$-h/c activity also directly stimulated autophagy activation. Thus $\beta$-h/c appears to be a key mediator in provoking an acute autophagic response in the brain endothelium and may be an important contributor to disease progression. Whether this

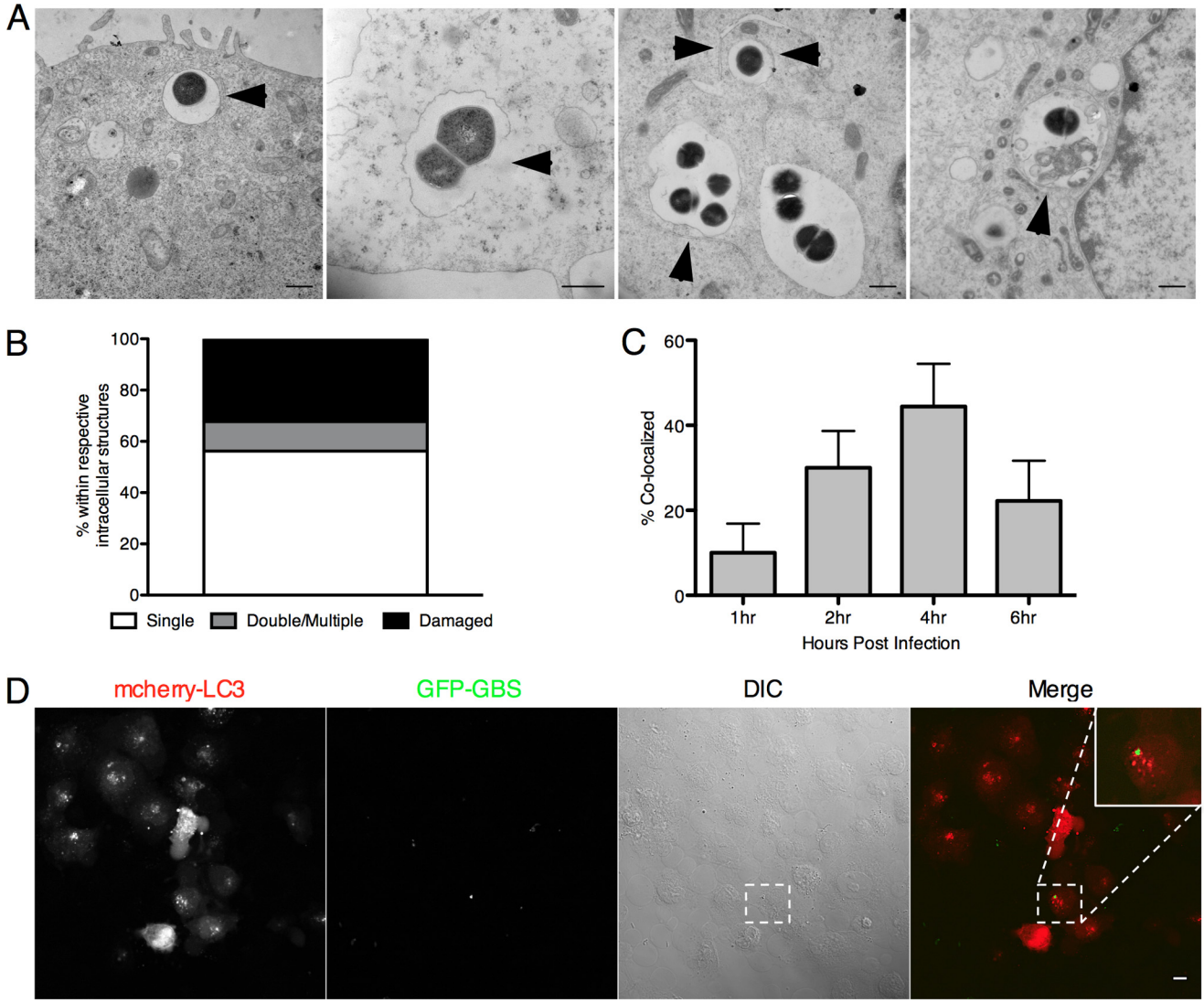


FIGURE 8. **Examination of the intracellular localization and LC3 co-localization of GBS.** *A* and *B*, transmission electron microscopy of intracellular GBS COH1 4 h after hBMEC infection (m.o.i. = 10). Intracellular bacteria were quantified according to the intracellular structure in which they resided ($n = 25$). Bacteria are present in membrane-bound vesicles, damaged membranes, multiple membranes, and putative autophagic structures as indicated by *arrowheads*. *Scale bar*, 500 nm. *C*, transfection of an mCherry-LC3 plasmid into hBMECs was performed as described under "Experimental Procedures." hBMECs were infected with GFP COH1 WT for 4 h prior to treatment with extracellular antibiotics 1, 2, 4, and 6 h postinfection. Quantification of the amount of GFP COH1 WT co-localizing with mCherry-LC3 was gathered by counting at least 100 cells with intracellular GBS, and data are means ± S.E. from a representative experiment performed in triplicate. *D*, representative confocal microscopic images from 4 h postinfection. *Scale bar*, 10 $\mu$m. *Error bars* represent S.D. *DIC*, differential interference contrast.

action is elicited by direct interaction of the toxin with endothelial signal transduction systems or activation is a secondary result of cellular injury that is mediated by the toxin remains to be elucidated. Recent studies investigating other bacterium-host interactions have shown that autophagy can be stimulated by toxins from *Vibrio cholerae* (56) and *B. anthracis* (57) and pore-forming toxins from GAS (58) and *S. aureus* (59). Interestingly, it has been recently suggested that hemolytic and cytolytic activity of GBS is due to the ornithine rhamnolipid pigment and not due to a pore-forming protein toxin (60). Furthermore, this associated carotenoid pigment has been shown to promote GBS intracellular survival in phagocytic cells (37). Thus it will be of interest to determine the exact mechanism of autophagy activation by the GBS $\beta$-h/c.

Research devoted toward the understanding of how antibacterial autophagy may defend against intracellular microbes has recently become of increasing interest. Classically cytosolic intracellular bacterial pathogens such as *Listeria*, *Shigella*, and GAS that disrupt phagosomal membranes and escape from these vesicles may be targeted for sequestration by autophagy, leading to their degradation (20, 61, 62). GAS escapes the endocytic pathway and enters the cytoplasm using a pore-forming cytolysin, streptolysin O (22, 63). Cytosolic GAS is then isolated into autophagosomes and rapidly undergoes lysosomal degradation. Autophagy may also target vesicular bacteria as is the case for *Mycobacterium* and *Salmonella* (20, 62). During infection of epithelial cells, *S. typhimurium* damages and escapes endosomal membranes, becomes ubiquitinated, and is recognized by autophagic adaptor proteins p62, nuclear dot protein 52, and optineurin for eventual binding to LC3 (64–66). Using TEM, we have visualized GBS mainly within single membrane-bound vesicles, which is consistent with early observations and

images of intracellular GBS in hBMECs (5). We have not observed GBS free in the cytosol even at later time points, although in some cases vesicle membranes appear to be disrupted (Fig. 8*A*). It has been observed that penicillin may gain access to the cytoplasm of eukaryotic cells (67), which may potentially kill GBS released into the cytoplasm. Although we cannot exclude this possibility, we should note that TEM analysis was performed in the absence of any antibiotics. Furthermore, we did observe a 30% increase in recovered GBS when using only gentamycin (data not shown), but this result is complicated by the fact that gentamycin alone was not as effective at killing extracellular GBS (data not shown). Our findings also suggest that intracellular GBS may traffic through other endosomal pathways. We have observed that GBS can traffic into Rab5- and Rab7-positive endosomes (data not shown), which is consistent with our TEM results suggesting the involvement of the endocytic pathway. The exact mechanisms and key players for recognition of intracellular vesicular GBS are incompletely understood as is the question of whether the β-h/c toxin is responsible for the vacuolar membrane damage we observed by TEM.

Pathogenic bacteria that survive within host cells utilize different strategies to avoid being killed in an autophagolysosome (68). These defensive mechanisms include resistance to autophagic engulfment, disruption of trafficking to the lysosome, and resistance to lysosomal killing. *S. typhimurium* has the capacity to survive and replicate intracellularly due to modulation of amino acid starvation-triggered mTOR inhibition that activates autophagy (69, 70). Recently, it has been reported that a clinically relevant serotype of GAS is able to degrade adaptor proteins, including p62, through secretion of a surface-associated protease, SpeB, thereby allowing GAS to persist in the cytoplasm (67). Other pathogens such as *S. flexneri* and *L. monocytogenes* avoid autophagic recognition by producing virulence factors that bind key autophagy-related proteins such as ATG5 and the ARP2/3 complex, thereby allowing for intracellular persistence and dissemination (46, 71, 72). Although our results demonstrate that autophagy is activated in BBB endothelium and host factors such as ATG5 and ATG12 contribute to bacterial clearance, GBS is not completely eliminated.

TEM analysis suggests that GBS is not readily sequestered in autophagosomes; however, up to ~40% of intracellular GBS co-localized with LC3 at 4 h postinfection (Fig. 8*C*). It has been demonstrated that LC3 can also be recruited to single membrane phagosomes or vesicles to assist in lysosomal fusion in a process denoted as LC3-associated phagocytosis (LAP) (73–76). Pathogens such as *Burkholderia pseudomallei* and *Mycobacterium marinum* have elicited LAP features in RAW264.7-GFP-LC3 macrophages (77–79). There is no clear indicator of LAP; however, there has been a universal consensus that the ATG5-ATG12-ATG16L1 complex is required for LAP induction (75, 80, 81). Defining whether macroautophagy or LAP occurs in the case of pathogen invasion has yet to be differentiated using GFP-conjugated LC3, but modulation of a subset of ATG proteins such as ATG5 and electron microscopic analysis of membrane-bound bacteria have been able to shed light on these subtle differences. Interestingly, inactivation of the ULK1-interacting protein FIP200, which is essential for the formation of the isolation membrane during autophagy but not recruitment of LC3 to membranes, did not impact recovery of intracellular GBS. This suggests that LAP may be critical for directing GBS to degradative compartments. Future studies are aimed to further elucidate the contribution of LAP to GBS uptake and intracellular trafficking.

In summary, we have demonstrated for the first time that the BBB endothelium activates autophagy in response to the meningeal pathogen GBS. We present evidence that this pathway may contribute to host cellular defense by controlling the intracellular pool of GBS. In addition, we have identified the GBS pore-forming toxin as the molecular trigger for autophagy activation. However, it will be important to investigate the autophagy adaptor proteins involved in the recognition of intracellular GBS, the impact of infection on autophagic flux, and whether other bacterial factors promote autophagy evasion and GBS intracellular survival. Ongoing studies on the modulation of host autophagy by meningeal pathogens are critical for understanding the host defense of the BBB and developing preventative therapies for CNS infection.

*Acknowledgments—We thank Monique Stins and Kwang Sik Kim for providing hBMECs, Noboru Mizushima for providing the ATG5 knock-out mouse embryonic fibroblasts and permission to use GFP-LC3 mice, Albert La Spada for providing the GFP-LC3 mice, Victor Nizet and John Buchanan for providing the GFP expression plasmid, Rick Sayen and Celia Ebrahimi for technical assistance, and Steve Barlow for providing assistance with electron microscopy. All animal experiments were approved by Institutional Animal Care and Use Committee at San Diego State University Protocol APF 13-07-011D and performed using accepted veterinary standards.*

## REFERENCES

1. Maisey, H. C., Doran, K. S., and Nizet, V. (2008) Recent advances in understanding the molecular basis of group B *Streptococcus* virulence. *Expert Rev. Mol. Med.* **10,** e27
2. Edwards, M. S., and Baker, C. J. (2005) Group B streptococcal infections in elderly adults. *Clin. Infect. Dis.* **41,** 839–847
3. Betz, A. L. (1985) Epithelial properties of brain capillary endothelium. *Fed. Proc.* **44,** 2614–2615
4. Betz, A. L., and Goldstein, G. W. (1986) Specialized properties and solute transport in brain capillaries. *Annu. Rev. Physiol.* **48,** 241–250
5. Nizet, V., Kim, K. S., Stins, M., Jonas, M., Chi, E. Y., Nguyen, D., and Rubens, C. E. (1997) Invasion of brain microvascular endothelial cells by group B streptococci. *Infect. Immun.* **65,** 5074–5081
6. Doran, K. S., Liu, G. Y., and Nizet, V. (2003) Group B streptococcal β-hemolysin/cytolysin activates neutrophil signaling pathways in brain endothelium and contributes to development of meningitis. *J. Clin. Investig.* **112,** 736–744
7. Lembo, A., Gurney, M. A., Burnside, K., Banerjee, A., de los Reyes, M., Connelly, J. E., Lin, W. J., Jewell, K. A., Vo, A., Renken, C. W., Doran, K. S., and Rajagopal, L. (2010) Regulation of CovR expression in group B *Streptococcus* impacts blood-brain barrier penetration. *Mol. Microbiol.* **77,** 431–443
8. Doran, K. S., Engelson, E. J., Khosravi, A., Maisey, H. C., Fedtke, I., Equils, O., Michelsen, K. S., Arditi, M., Peschel, A., and Nizet, V. (2005) Blood-brain barrier invasion by group B *Streptococcus* depends upon proper cell-surface anchoring of lipoteichoic acid. *J. Clin. Investig.* **115,** 2499–2507
9. Seo, H. S., Mu, R., Kim, B. J., Doran, K. S., and Sullam, P. M. (2012) Binding of glycoprotein Srr1 of *Streptococcus agalactiae* to fibrinogen promotes attachment to brain endothelium and the development of meningitis.

*PLoS Pathog.* **8,** e1002947
10. van Sorge, N. M., Quach, D., Gurney, M. A., Sullam, P. M., Nizet, V., and Doran, K. S. (2009) The group B streptococcal serine-rich repeat 1 glycoprotein mediates penetration of the blood-brain barrier. *J. Infect. Dis.* **199,** 1479–1487
11. Tenenbaum, T., Bloier, C., Adam, R., Reinscheid, D. J., and Schroten, H. (2005) Adherence to and invasion of human brain microvascular endothelial cells are promoted by fibrinogen-binding protein FbsA of *Streptococcus agalactiae*. *Infect. Immun.* **73,** 4404–4409
12. Tenenbaum, T., Spellerberg, B., Adam, R., Vogel, M., Kim, K. S., and Schroten, H. (2007) *Streptococcus agalactiae* invasion of human brain microvascular endothelial cells is promoted by the laminin-binding protein Lmb. *Microbes Infect.* **9,** 714–720
13. Tazi, A., Disson, O., Bellais, S., Bouaboud, A., Dmytruk, N., Dramsi, S., Mistou, M. Y., Khun, H., Mechler, C., Tardieux, I., Trieu-Cuot, P., Lecuit, M., and Poyart, C. (2010) The surface protein HvgA mediates group B *Streptococcus* hypervirulence and meningeal tropism in neonates. *J. Exp. Med.* **207,** 2313–2322
14. Chang, Y. C., Wang, Z., Flax, L. A., Xu, D., Esko, J. D., Nizet, V., and Baron, M. J. (2011) Glycosaminoglycan binding facilitates entry of a bacterial pathogen into central nervous systems. *PLoS Pathog.* **7,** e1002082
15. Banerjee, A., Kim, B. J., Carmona, E. M., Cutting, A. S., Gurney, M. A., Carlos, C., Feuer, R., Prasadarao, N. V., and Doran, K. S. (2011) Bacterial pili exploit integrin machinery to promote immune activation and efficient blood-brain barrier penetration. *Nat. Commun.* **2,** 462
16. Maisey, H. C., Hensler, M., Nizet, V., and Doran, K. S. (2007) Group B streptococcal pilus proteins contribute to adherence to and invasion of brain microvascular endothelial cells. *J. Bacteriol.* **189,** 1464–1467
17. Levine, B., Mizushima, N., and Virgin, H. W. (2011) Autophagy in immunity and inflammation. *Nature* **469,** 323–335
18. Levine, B., and Deretic, V. (2007) Unveiling the roles of autophagy in innate and adaptive immunity. *Nat. Rev. Immunol.* **7,** 767–777
19. Mizushima, N., Yoshimori, T., and Ohsumi, Y. (2011) The role of Atg proteins in autophagosome formation. *Annu. Rev. Cell Dev. Biol.* **27,** 107–132
20. Huang, J., and Brumell, J. H. (2009) Autophagy in immunity against intracellular bacteria. *Curr. Top. Microbiol. Immunol.* **335,** 189–215
21. Mostowy, S., Sancho-Shimizu, V., Hamon, M. A., Simeone, R., Brosch, R., Johansen, T., and Cossart, P. (2011) p62 and NDP52 proteins target intracytosolic *Shigella* and *Listeria* to different autophagy pathways. *J. Biol. Chem.* **286,** 26987–26995
22. Nakagawa, I., Amano, A., Mizushima, N., Yamamoto, A., Yamaguchi, H., Kamimoto, T., Nara, A., Funao, J., Nakata, M., Tsuda, K., Hamada, S., and Yoshimori, T. (2004) Autophagy defends cells against invading group A *Streptococcus*. *Science* **306,** 1037–1040
23. Thurston, T. L., Ryzhakov, G., Bloor, S., von Muhlinen, N., and Randow, F. (2009) The TBK1 adaptor and autophagy receptor NDP52 restricts the proliferation of ubiquitin-coated bacteria. *Nat. Immunol.* **10,** 1215–1221
24. Knodler, L. A., and Celli, J. (2011) Eating the strangers within: host control of intracellular bacteria via xenophagy. *Cell. Microbiol.* **13,** 1319–1327
25. Cataldi, A., Labruyère, E., and Mock, M. (1990) Construction and characterization of a protective antigen-deficient *Bacillus anthracis* strain. *Mol. Microbiol.* **4,** 1111–1117
26. Pattee, P. A. (1981) Distribution of Tn551 insertion sites responsible for auxotrophy on the *Staphylococcus aureus* chromosome. *J. Bacteriol.* **145,** 479–488
27. Wilkinson, H. W. (1977) Nontypable group B streptococci isolated from human sources. *J. Clin. Microbiol.* **6,** 183–184
28. Wilson, C. B., and Weaver, W. M. (1985) Comparative susceptibility of group B streptococci and *Staphylococcus aureus* to killing by oxygen metabolites. *J. Infect. Dis.* **152,** 323–329
29. Pritzlaff, C. A., Chang, J. C., Kuo, S. P., Tamura, G. S., Rubens, C. E., and Nizet, V. (2001) Genetic basis for the β-haemolytic/cytolytic activity of group B *Streptococcus*. *Mol. Microbiol.* **39,** 236–247
30. Maisey, H. C., Quach, D., Hensler, M. E., Liu, G. Y., Gallo, R. L., Nizet, V., and Doran, K. S. (2008) A group B streptococcal pilus protein promotes phagocyte resistance and systemic virulence. *FASEB J.* **22,** 1715–1724
31. Ebrahimi, C. M., Kern, J. W., Sheen, T. R., Ebrahimi-Fardooee, M. A., van Sorge, N. M., Schneewind, O., and Doran, K. S. (2009) Penetration of the blood-brain barrier by *Bacillus anthracis* requires the pXO1-encoded BslA protein. *J. Bacteriol.* **191,** 7165–7173
32. Sheen, T. R., Ebrahimi, C. M., Hiemstra, I. H., Barlow, S. B., Peschel, A., and Doran, K. S. (2010) Penetration of the blood-brain barrier by *Staphylococcus aureus*: contribution of membrane-anchored lipoteichoic acid. *J. Mol. Med.* **88,** 633–639
33. Stins, M. F., Prasadarao, N. V., Zhou, J., Arditi, M., and Kim, K. S. (1997) Bovine brain microvascular endothelial cells transfected with SV40-large T antigen: development of an immortalized cell line to study pathophysiology of CNS disease. *In Vitro Cell. Dev. Biol. Anim.* **33,** 243–247
34. Kuma, A., Hatano, M., Matsui, M., Yamamoto, A., Nakaya, H., Yoshimori, T., Ohsumi, Y., Tokuhisa, T., and Mizushima, N. (2004) The role of autophagy during the early neonatal starvation period. *Nature* **432,** 1032–1036
35. Mizushima, N., Yamamoto, A., Hatano, M., Kobayashi, Y., Kabeya, Y., Suzuki, K., Tokuhisa, T., Ohsumi, Y., and Yoshimori, T. (2001) Dissection of autophagosome formation using Apg5-deficient mouse embryonic stem cells. *J. Cell Biol.* **152,** 657–668
36. Hamacher-Brady, A., Brady, N. R., and Gottlieb, R. A. (2006) Enhancing macroautophagy protects against ischemia/reperfusion injury in cardiac myocytes. *J. Biol. Chem.* **281,** 29776–29787
37. Liu, G. Y., Doran, K. S., Lawrence, T., Turkson, N., Puliti, M., Tissi, L., and Nizet, V. (2004) Sword and shield: linked group B streptococcal β-hemolysin/cytolysin and carotenoid pigment function to subvert host phagocyte defense. *Proc. Natl. Acad. Sci. U.S.A.* **101,** 14491–14496
38. Nizet, V., Gibson, R. L., Chi, E. Y., Framson, P. E., Hulse, M., and Rubens, C. E. (1996) Group B streptococcal β-hemolysin expression is associated with injury of lung epithelial cells. *Infect. Immun.* **64,** 3818–3826
39. Mizushima, N., Yamamoto, A., Matsui, M., Yoshimori, T., and Ohsumi, Y. (2004) *In vivo* analysis of autophagy in response to nutrient starvation using transgenic mice expressing a fluorescent autophagosome marker. *Mol. Biol. Cell* **15,** 1101–1111
40. Tanida, I., Ueno, T., and Kominami, E. (2008) LC3 and autophagy. *Methods Mol. Biol.* **445,** 77–88
41. Yitzhaki, S., Huang, C., Liu, W., Lee, Y., Gustafsson, A. B., Mentzer, R. M., Jr., and Gottlieb, R. A. (2009) Autophagy is required for preconditioning by the adenosine A1 receptor-selective agonist CCPA. *Basic Res. Cardiol.* **104,** 157–167
42. Bjørkøy, G., Lamark, T., Pankiv, S., Øvervatn, A., Brech, A., and Johansen, T. (2009) Monitoring autophagic degradation of p62/SQSTM1. *Methods Enzymol.* **452,** 181–197
43. Birgisdottir, Å. B., Lamark, T., and Johansen, T. (2013) The LIR motif—crucial for selective autophagy. *J. Cell Sci.* **126,** 3237–3247
44. Dupont, N., Lacas-Gervais, S., Bertout, J., Paz, I., Freche, B., Van Nhieu, G. T., van der Goot, F. G., Sansonetti, P. J., and Lafont, F. (2009) *Shigella* phagocytic vacuolar membrane remnants participate in the cellular response to pathogen invasion and are regulated by autophagy. *Cell Host Microbe* **6,** 137–149
45. Noda, N. N., Ohsumi, Y., and Inagaki, F. (2010) Atg8-family interacting motif crucial for selective autophagy. *FEBS Lett.* **584,** 1379–1385
46. Yoshikawa, Y., Ogawa, M., Hain, T., Yoshida, M., Fukumatsu, M., Kim, M., Mimuro, H., Nakagawa, I., Yanagawa, T., Ishii, T., Kakizuka, A., Sztul, E., Chakraborty, T., and Sasakawa, C. (2009) *Listeria monocytogenes* ActA-mediated escape from autophagic recognition. *Nat. Cell Biol.* **11,** 1233–1240
47. Pankiv, S., Clausen, T. H., Lamark, T., Brech, A., Bruun, J. A., Outzen, H., Øvervatn, A., Bjørkøy, G., and Johansen, T. (2007) p62/SQSTM1 binds directly to Atg8/LC3 to facilitate degradation of ubiquitinated protein aggregates by autophagy. *J. Biol. Chem.* **282,** 24131–24145
48. Mizushima, N. (2009) Methods for monitoring autophagy using Gfp-Lc3 transgenic mice. *Methods Enzymol.* **452,** 13–23
49. Cai, Z., Zhao, B., Li, K., Zhang, L., Li, C., Quazi, S. H., and Tan, Y. (2012) Mammalian target of rapamycin: a valid therapeutic target through the autophagy pathway for Alzheimer's disease? *J. Neurosci. Res.* **90,** 1105–1118
50. Noda, T., and Ohsumi, Y. (1998) Tor, a phosphatidylinositol kinase homologue, controls autophagy in yeast. *J. Biol. Chem.* **273,** 3963–3966

51. Ravikumar, B., Duden, R., and Rubinsztein, D. C. (2002) Aggregate-prone proteins with polyglutamine and polyalanine expansions are degraded by autophagy. *Hum. Mol. Genet.* **11,** 1107–1117
52. Yamamoto, A., Tagawa, Y., Yoshimori, T., Moriyama, Y., Masaki, R., and Tashiro, Y. (1998) Bafilomycin A1 prevents maturation of autophagic vacuoles by inhibiting fusion between autophagosomes and lysosomes in rat hepatoma cell line, H-4-II-E cells. *Cell Struct. Funct.* **23,** 33–42
53. Hara, T., Takamura, A., Kishi, C., Iemura, S., Natsume, T., Guan, J. L., and Mizushima, N. (2008) FIP200, a ULK-interacting protein, is required for autophagosome formation in mammalian cells. *J. Cell Biol.* **181,** 497–510
54. Doran, K. S., Chang, J. C., Benoit, V. M., Eckmann, L., and Nizet, V. (2002) Group B streptococcal β-hemolysin/cytolysin promotes invasion of human lung epithelial cells and the release of interleukin-8. *J. Infect. Dis.* **185,** 196–203
55. Sagar, A., Klemm, C., Hartjes, L., Mauerer, S., van Zandbergen, G., and Spellerberg, B. (2013) The β-hemolysin and intracellular survival of *Streptococcus agalactiae* in human macrophages. *PLoS One* **8,** e60160
56. Gutierrez, M. G., Saka, H. A., Chinen, I., Zoppino, F. C., Yoshimori, T., Bocco, J. L., and Colombo, M. I. (2007) Protective role of autophagy against *Vibrio cholerae* cytolysin, a pore-forming toxin from *V. cholerae*. *Proc. Natl. Acad. Sci. U.S.A.* **104,** 1829–1834
57. Ebrahimi, C. M., Sheen, T. R., Renken, C. W., Gottlieb, R. A., and Doran, K. S. (2011) Contribution of lethal toxin and edema toxin to the pathogenesis of anthrax meningitis. *Infect. Immun.* **79,** 2510–2518
58. O'Seaghdha, M., and Wessels, M. R. (2013) Streptolysin O and its co-toxin NAD-glycohydrolase protect group A *Streptococcus* from xenophagic killing. *PLoS Pathog.* **9,** e1003394
59. Mestre, M. B., Fader, C. M., Sola, C., and Colombo, M. I. (2010) α-Hemolysin is required for the activation of the autophagic pathway in *Staphylococcus aureus*-infected cells. *Autophagy* **6,** 110–125
60. Whidbey, C., Harrell, M. I., Burnside, K., Ngo, L., Becraft, A. K., Iyer, L. M., Aravind, L., Hitti, J., Waldorf, K. M., and Rajagopal, L. (2013) A hemolytic pigment of group B *Streptococcus* allows bacterial penetration of human placenta. *J. Exp. Med.* **210,** 1265–1281
61. Mostowy, S. (2013) Autophagy and bacterial clearance: a not so clear picture. *Cell. Microbiol.* **15,** 395–402
62. Huang, J., and Brumell, J. H. (2014) Bacteria-autophagy interplay: a battle for survival. *Nat. Rev. Microbiol.* **12,** 101–114
63. Sakurai, A., Maruyama, F., Funao, J., Nozawa, T., Aikawa, C., Okahashi, N., Shintani, S., Hamada, S., Ooshima, T., and Nakagawa, I. (2010) Specific behavior of intracellular *Streptococcus pyogenes* that has undergone autophagic degradation is associated with bacterial streptolysin O and host small G proteins Rab5 and Rab7. *J. Biol. Chem.* **285,** 22666–22675
64. Thurston, T. L., Wandel, M. P., von Muhlinen, N., Foeglein, A., and Randow, F. (2012) Galectin 8 targets damaged vesicles for autophagy to defend cells against bacterial invasion. *Nature* **482,** 414–418
65. Wild, P., Farhan, H., McEwan, D. G., Wagner, S., Rogov, V. V., Brady, N. R., Richter, B., Korac, J., Waidmann, O., Choudhary, C., Dötsch, V., Bumann, D., and Dikic, I. (2011) Phosphorylation of the autophagy receptor optineurin restricts *Salmonella* growth. *Science* **333,** 228–233
66. Zheng, Y. T., Shahnazari, S., Brech, A., Lamark, T., Johansen, T., and Brumell, J. H. (2009) The adaptor protein p62/SQSTM1 targets invading bacteria to the autophagy pathway. *J. Immunol.* **183,** 5909–5916
67. Barnett, T. C., Liebl, D., Seymour, L. M., Gillen, C. M., Lim, J. Y., Larock, C. N., Davies, M. R., Schulz, B. L., Nizet, V., Teasdale, R. D., and Walker, M. J. (2013) The globally disseminated M1T1 clone of group A *Streptococcus* evades autophagy for intracellular replication. *Cell Host Microbe* **14,** 675–682
68. Duclos, S., and Desjardins, M. (2000) Subversion of a young phagosome: the survival strategies of intracellular pathogens. *Cell. Microbiol.* **2,** 365–377
69. Birmingham, C. L., Smith, A. C., Bakowski, M. A., Yoshimori, T., and Brumell, J. H. (2006) Autophagy controls *Salmonella* infection in response to damage to the *Salmonella*-containing vacuole. *J. Biol. Chem.* **281,** 11374–11383
70. Tattoli, I., Sorbara, M. T., Vuckovic, D., Ling, A., Soares, F., Carneiro, L. A., Yang, C., Emili, A., Philpott, D. J., and Girardin, S. E. (2012) Amino acid starvation induced by invasive bacterial pathogens triggers an innate host defense program. *Cell Host Microbe* **11,** 563–575
71. Ogawa, M., Yoshimori, T., Suzuki, T., Sagara, H., Mizushima, N., and Sasakawa, C. (2005) Escape of intracellular *Shigella* from autophagy. *Science* **307,** 727–731
72. Birmingham, C. L., Canadien, V., Gouin, E., Troy, E. B., Yoshimori, T., Cossart, P., Higgins, D. E., and Brumell, J. H. (2007) *Listeria monocytogenes* evades killing by autophagy during colonization of host cells. *Autophagy* **3,** 442–451
73. Mehta, P., Henault, J., Kolbeck, R., and Sanjuan, M. A. (2014) Noncanonical autophagy: one small step for LC3, one giant leap for immunity. *Curr. Opin. Immunol.* **26,** 69–75
74. Romao, S., and Münz, C. (2014) LC3-associated phagocytosis. *Autophagy* **10,** 526–528
75. Sanjuan, M. A., Dillon, C. P., Tait, S. W., Moshiach, S., Dorsey, F., Connell, S., Komatsu, M., Tanaka, K., Cleveland, J. L., Withoff, S., and Green, D. R. (2007) Toll-like receptor signalling in macrophages links the autophagy pathway to phagocytosis. *Nature* **450,** 1253–1257
76. Deretic, V., Saitoh, T., and Akira, S. (2013) Autophagy in infection, inflammation and immunity. *Nat. Rev. Immunol.* **13,** 722–737
77. Gong, L., Cullinane, M., Treerat, P., Ramm, G., Prescott, M., Adler, B., Boyce, J. D., and Devenish, R. J. (2011) The *Burkholderia pseudomallei* type III secretion system and BopA are required for evasion of LC3-associated phagocytosis. *PLoS One* **6,** e17852
78. Lerena, M. C., and Colombo, M. I. (2011) *Mycobacterium marinum* induces a marked LC3 recruitment to its containing phagosome that depends on a functional ESX-1 secretion system. *Cell. Microbiol.* **13,** 814–835
79. Li, X., Prescott, M., Adler, B., Boyce, J. D., and Devenish, R. J. (2013) Beclin 1 is required for starvation-enhanced, but not rapamycin-enhanced, LC3-associated phagocytosis of *Burkholderia pseudomallei* in RAW 264.7 cells. *Infect. Immun.* **81,** 271–277
80. Huang, J., Canadien, V., Lam, G. Y., Steinberg, B. E., Dinauer, M. C., Magalhaes, M. A., Glogauer, M., Grinstein, S., and Brumell, J. H. (2009) Activation of antibacterial autophagy by NADPH oxidases. *Proc. Natl. Acad. Sci. U.S.A.* **106,** 6226–6231
81. Lai, S. C., and Devenish, R. J. (2012) LC3-associated phagocytosis (LAP): connections with host autophagy. *Cells* **1,** 396–408